Understanding the role of the Q338H MUTYH variant in oxidative damage repair

Eleonora Turco[1], Ilenia Ventura[1], Anna Minoprio[1], Maria Teresa Russo[1], Paola Torreri[2], Paolo Degan[3], Sara Molatore[4], Guglielmina Nadia Ranzani[4], Margherita Bignami[1,*] and Filomena Mazzei[1,*]

[1]Department of Environment and Primary Prevention, Istituto Superiore di Sanità, 00161 Roma, Italy, [2]National Center for Rare Diseases, Istituto Superiore di Sanità, 00161 Roma, Italy, [3]IRCCS Azienda Ospedaliera Universitaria San Martino-Istituto Nazionale per la Ricerca sul Cancro, 16123 Genova, Italy and [4]Department of Genetics and Microbiology, University of Pavia, 27100 Pavia, Italy

ABSTRACT

The MUTYH DNA–glycosylase is indirectly engaged in the repair of the miscoding 7,8-dihydro-8-oxo-2′-deoxyguanine (8-oxodG) lesion by removing adenine erroneously incorporated opposite the oxidized purine. Inherited biallelic mutations in the *MUTYH* gene are responsible for a recessive syndrome, the MUTYH-associated polyposis (MAP), which confers an increased risk of colorectal cancer. In this study, we functionally characterized the Q338H variant using recombinant proteins, as well as cell-based assays. This is a common variant among human colorectal cancer genes, which is generally considered, unrelated to the MAP phenotype but recently indicated as a low-penetrance allele. We demonstrate that the Q338H variant retains a wild-type DNA–glycosylase activity *in vitro,* but it shows a reduced ability to interact with the replication sensor RAD9:RAD1:HUS1 (9–1–1) complex. In comparison with *Mutyh*^{−/−} mouse embryo fibroblasts expressing a wild-type *MUTYH* cDNA, the expression of Q338H variant was associated with increased levels of DNA 8-oxodG, hypersensitivity to oxidant and accumulation of the population in the S phase of the cell cycle. Thus, an inefficient interaction of MUTYH with the 9–1–1 complex leads to a repair-defective phenotype, indicating that a proper communication between MUTYH enzymatic function and the S phase checkpoint is needed for effective repair of oxidative damage.

INTRODUCTION

The human DNA–glycosylase MUTYH is involved in the base excision repair (BER) of 7,8-dihydro-8-oxo-2′-deoxyguanine (8-oxodG) by preventing the onset of G to T transversion mutations (1,2). MUTYH chiefly operates on duplex DNA substrates containing 8-oxodG:A mispairs by removing adenine erroneously incorporated by DNA polymerases (3,4), and the resulting abasic site is subsequently incised by the AP-endonuclease1 (APE1). DNA repair polymerases, flap endonuclease 1 (FEN1) and finally DNA ligase 1 (LIG1) bring the repair process to completion (5–7). MUTYH activity is concentrated during the S phase of the cell cycle, where it reaches maximum levels of expression (8). MUTYH is also known to physically interact with the MutS homolog 6 (MSH6) mismatch repair (MMR) protein (9), the replication protein-A (RP-A) (5) and the proliferating cell nuclear antigen (PCNA) (10), the latter allowing the recognition of the newly synthesized strand to be repaired.

Loss or reduction of MUTYH activity is responsible for the occurrence of the recessively inherited adenomatous polyposis disease (MUTYH-associated polyposis, MAP), which predisposes to colorectal cancer (11,12). Several variants have been identified in MAP patients (13), and the mechanism underlying a defective enzymatic function has been extensively investigated by monitoring the DNA–glycosylase activity on synthetic DNA substrates. Recombinant bacterial (11), human (14–19), murine (20–22) MUTY/MUTYH proteins, as well as lysates derived from lymphoblastoid cell lines from MAP patients, (23,24) were used. The most common variants have been found totally or partially devoid of DNA–glycosylase activity, and the adenine removal capability is generally taken as a functional biomarker.

However, because of the large number of protein–protein interactions involving MUTYH, the protein interaction network should also be investigated as far as the functional activity of the protein is concerned. DNA repair during the S phase is a challenging task, and cell-cycle regulation (namely, its delay or arrest) is required to allow DNA replication with high fidelity (25). In particular, stalling of replication forks, which occurs when these encounter an obstacle in DNA template, such as damaged bases, DNA repair intermediates or DNA–proteins complexes, is dealt in eukaryotes by a complex machinery that detects these unusual structures and eventually delays cell-cycle progression, allowing time to repair DNA damage and/or trigger apoptosis. In humans, the ternary RAD9:RAD1:HUS1 (henceforth 9–1–1) complex has been characterized as replication checkpoint sensor that targets to the nucleus in response to oxidative stress through the activation of the ataxia telangiectasia and Rad3 related protein (ATR)-serine/threonine-protein kinase1 (CHK1) pathway. The 9–1–1 complex forms a heterotrimeric complex (26,27) that resembles the PCNA structure and has been found to physically interact with MUTYH (28,29) through the HUS1 component at residues 309–374 of MUTYH [according to the new nomenclature, (13)] and slightly stimulates MUTYH DNA–glycosylase activity (28). This latter characteristic is shared not only by many other BER proteins, such as APE1 (30), polymerase β (POLβ)(31), FEN1 (32,33), LIG1 (34,35), but also by other DNA glycosylases, such as 8-oxoG DNA glycosylase1 (OGG1) (36), thymine DNA glycosylase (TDG) (37) and endonuclease VIII-like glycosylase1 (NEIL1) (38). Together with a significant interaction with RP-A (39), a relevant role for the 9–1–1 complex has also been found in MMR, another DNA repair pathway active at replication (40).

The Q338H variant is generally considered as a common polymorphism without a significant clinical impact (11,12), although there is some disagreement on a possible moderate impairment of its DNA–glycosylase activity (16,22,41,42). The 338 residue position in which glutamine is substituted with histidine is far from the catalytic site (43,29), but it is located in the interconnecting domain (IDC) involved in the interaction with the HUS1 component of the 9–1–1 complex (29). In this study, we performed a biochemical characterization of this MUTYH polymorphic variant and investigated whether the Q338H mutation might affect this interaction. Although DNA binding and DNA–glycosylase activity of the purified recombinant Q338H did not differ significantly from the wild-type protein, a diminished interaction with the 9–1–1 complex was established by pull-down assays. In addition, when wild-type and Q338H cDNAs were expressed in *Mutyh$^{-/-}$* mouse embryo fibroblasts (MEFs), increased sensitivity to oxidant treatment, alterations in the progression of the S phase of the cell cycle and defective removal of DNA damage were found to be associated with Q338H expression.

These results suggest that the defective ability of Q338H variant to interact with checkpoint proteins recruited at DNA damaged sites might affect the timing and extent of DNA repair, ultimately causing a block of DNA synthesis leading to cell death.

MATERIALS AND METHODS

DNA substrates

A 30mer oligonucleotide (A-strand), 3′-end labelled with 6-carboxyfluorescein (6-FAM) and high-performance liquid chromatography (HPLC) purified (5′-GCA AAG AAC TTA TAG **A**CC CCC TTG AGC ACA CAG AGG-3′–6-FAM), was annealed to the complementary strand containing a single 8-oxodG and was used as substrate in the DNA–glycosylase assay. For surface plasmon resonance (SPR) measurements, the A-strand was the 48mer 5′-GTC GTG GAC TAG GCA AAG AAC TTA TAG **A**GC CAC TTG AGC ACA CAG AGG-3′, and a 14mer biotinylated DNA (5′-CTA GTC CAC GAC TTT TTT TT-3′–Biotin) was the target DNA immobilized on the sensor chip. All oligonucleotides were from Thermo Fisher Scientific (Thermo Fisher Scientific GmbH, Ulm, Germany).

Recombinant maltose binding protein (MBP)–MUTYH expression and purification

The *MUTYH* cDNA was amplified by polymerase chain reaction using primers containing BamHI (primer forward) and HindIII (primer reverse) restriction sites and inserted in a pMAL-c4E vector (NEB), which was then used to transform the *Escherichia coli* strain BL21 CodonPlus (DE3) RIPL (Stratagene, La Jolla, CA, USA). Mutation at codon 338 was generated by the QuikChange^{TM} Site-Directed Mutagenesis Kit (Stratagene, La Jolla, CA, USA). The competent cells were transformed with the pMAL-MUTYH vector using standard heat-shock procedures, and colonies were selected using 100 μg/μl of ampicillin and 30 μg/μl of chloramphenicol on Luria broth (LB) agar plates. Cultures were grown at 37°C in LB medium with 5 g/l of glucose to an OD$_{600nm}$ = 0.6 and then induced by the addition of a final concentration of 0.4 mM isopropyl-β-D-thiogalactopyranoside for 3 h at 25°C. Cells were harvested and resuspended in phosphate-buffered saline (PBS) (1/40th of culture volume). In all, 5 mM dithiothreitol (DTT), 1 mg/ml of lysozyme and protease inhibitors were added to the cell suspension and incubated for 30 min on ice. Cell lysis was completed by three freeze and thaw cycles and addition of 5 μg/ml DNase. Cellular debris were removed by centrifugation, and the supernatant was loaded on a chromatographic column packed with amylose resin. The recombinant fusion protein was eluted in 10 mM Tris–HCl, pH 7.5, 10 mM maltose buffer and analysed by sodium dodecyl sulphate–polyacrylamide gel electrophoresis (SDS–PAGE). Comassie staining of the gel was then performed (Supplementary Figure S1). Protein recovery was evaluated by gel analysis by *ImageJ* software, available free online at the NIH website (http://rsb.info.nih.gov/).

MUTYH active fraction evaluation and DNA–glycosylase activity assay

The DNA–glycosylase activity was measured by reacting the DNA substrate, containing a single 8-oxodG:A mispair, with wild-type or Q338H MBP–MUTYH protein at 37°C in 20 mM Tris–HCl, pH 8, 100 mM NaCl, 1 mM ethylenediaminetetraacetic acid (EDTA), 1 mM DTT and 0.1 mg/ml of bovine serum albumin buffer. The A-strand of the DNA substrate was 3′-end labelled with 6-FAM. The active site titration was performed by running time course kinetics of adenine removal using 10 nM DNA duplex substrate and a protein concentration able to produce ~20% of the product. Aliquots were collected at different time, and the reaction products were separated by PAGE. Data were fitted to the Equation (1)

$$(P) = A_o(1 - \exp(-k_B)t) + k_L t \tag{1}$$

where (P) is the cleavage product concentration at time t, (A_o) is the amplitude of the burst proportional to the active protein fraction concentration, (k_B) is the rate constant of the exponential phase and (k_L) the slope of the linear phase.

In single-turnover conditions ([MUTYH]»[DNA]), DNA substrate (2 nM) was reacted with an active protein (20 nM). Aliquots were withdrawn at different times, ranging from 30 s to 10 min, and reaction was stopped by addition of NaOH (80 mM) and heating at 90°C for 4 min. Reaction products were separated by denaturing PAGE, and data were analysed as reported earlier in the text. Data were fitted to Equation (2) to estimate the rate of product formation (k):

$$(P) = A_o(1 - \exp(-k_{ST}t)) \tag{2}$$

The DNA–glycosylase activity assay in the presence of APE1 was carried out by adding 1 U of APE1 enzyme (Trevigen, Gaithersburg, MD, USA) to the reaction mixture, containing the DNA substrate (10 nM) and MUTYH (5 nM, active fraction concentration), and allowing the reaction to proceed at 37°C for 1 h. Aliquots withdrawn at the time indicated in the legend to the figure were treated by alkali and analysed by PAGE.

Binding affinity measurements of wild-type and Q338H MUTYH to a DNA substrate by surface plasmon resonance

SPR analysis was performed using a Biacore X instrument (GE Healthcare, Uppsala, Sweden) with a streptavidin (SA) sensor chip at 25°C. The running buffer was 10 mM 4-(2 hydroxyethyl)-1-piperazineethansulfonic acid (HEPES), pH 7.4, 150 mM NaCl, 3.4 mM EDTA and 0.05% P20 surfactant (HBS-EP). Measurements were performed as previously described (18). Following the usual activation procedure of SA chip, carried out as recommended by the manufacturer, the immobilization of biotin–DNA sample was obtained at 25°C by injecting a single strand at low flow rate (2 μl/min). After extensive washing with HBS-EP buffer, duplex DNA substrate was injected at 2 μl/min to obtain ~100 response units (RU),

and the response was monitored as a function of time. Binding of wild-type and MUTYH variant was carried out by injecting 60 μl of serial dilutions of both proteins at 30 μl/min. The regeneration of the SA chip was obtained by short pulse of NaOH 35 mM. The SPR data were analysed using the 1:1 Langmuir model with the BIAevaluation software (GE Healthcare, Uppsala, Sweden).

Pull-down assays

HeLa cells were grown in low glucose Dulbecco's Modified Essential Medium supplemented with 10% fetal bovine serum, 100 U/ml of penicillin and 100 μg/ml of streptomycin (complete medium) at 37°C in 5% CO_2 atmosphere. Nuclear extracts were prepared as described by Klungland *et al.* (44). Wild-type and variant MBP–MUTYH proteins (5 μg) were incubated with HeLa nuclear extracts overnight at 4°C in HEPES–KOH 10 mM, pH 7.4, KCl 100 mM and $MgCl_2$ 10 mM buffer. The samples were then added to 30 μl of anti-MBP magnetic beads (1 mg/ml and binding capacity of 10 μg/mg) (New England BioLabs, Ipswich, MA, USA), pre-treated as described by manufacturer. After incubation, a magnet was applied, and supernatant was decanted. The procedure was repeated three times to remove aspecifically bound proteins. The bead pellets were resuspended in 40 μl of Laemnli buffer 3 × [187.5 mM Tris–HCl, pH 6.8, 6% (w/v) SDS, 30% glycerol, 150 mM DTT and 0.03% (w/v) bromophenol blue] and heated at 70°C for 5 min. Supernatants (20 μl) were loaded on an SDS–gel NuPAGE 4–12% (Novex, Invitrogen), and proteins were transferred to a nitrocellulose membrane for western blot analysis. Membranes were probed with primary antibodies against MUTYH (dilution 1:500, Abcam, UK), RAD9 (dilution 1:500, Abcam, UK) and HUS1 (dilution 1:10000, Abcam, UK). Secondary antibodies were horseradish peroxidase-conjugated antibodies (1:10000, Alexa, Invitrogen). Reactive proteins were detected by chemiluminescence with WesternBright ECL (Advansta, CA, USA) by using the ChemidocMP system (BioRad, Life Science).

Pull-down with purified 9–1–1 complex (Enzo Life Sciences, Farmingdale, NY, USA; purity >90%) was obtained by incubating at 4°C the recombinant complex (1 μg) with wild-type or Q338H MBP–MUTYH (300 ng), previously immobilized on the magnetic beads. The samples were then pulled down and analysed as described earlier in the text.

Cell cultures and DNA transfection

Immortalized MEFs derived from *Mutyh*$^{-/-}$ mice (45) grown in complete medium were transfected (Lipofectamine 2000; Invitrogen) with pWMv200-MUTYH vectors containing wild-type or variant *MUTYH* cDNA, constructed as previously reported (46), and selected for G418 (900 μg/ml) resistance. For western blot analyses, cell lysates were loaded on SDS–7.5% polyacrylamide gels, transferred to nitrocellulose membrane and incubated overnight with a rabbit polyclonal antibody against MUTYH (dilution 1:200, Novus Biologicals, Littleton, CO, USA). The antigen–antibody

complex was detected by incubation for 1 h at room temperature with the peroxidase-conjugated secondary anti-rabbit antibody (Alexa, Invitrogen).

Evaluation of cell survival and cell cycle analysis after KBrO$_3$ treatment

Cells (200/dish) were seeded in complete medium and exposed 24 h later to increasing concentrations of KBrO$_3$ in PBS and 20 mM HEPES (pH 7.4) for 30 min at 37°C. After 1 week, surviving colonies were fixed with ethanol, stained with Giemsa and counted. To determine the effects of KBrO$_3$ treatment on cell cycle progression, cells were plated (1×10^6) on Petri dishes and incubated with different doses of KBrO$_3$ for 30 min at 37°C. At different times from the end of the treatment, cells were harvested, suspended in ice cold 70% ethanol and frozen at -20°C. Before performing fluorescence-activated cell sorting (FACS) analyses, cells were incubated for 30 min at room temperature in a lysis buffer (0.1% trisodium citrate, 0.1% Triton and 10 μg/ml of RNase) containing propidium iodide (25 μg/ml). Flow cytofluorimeter measurements were performed by FACScan flow cytometer (Becton & Dickinson) and cell cycle analysis by ModFit LT software and Cell Quest.

The 8-OxodG evaluation

The 8-OxodG was measured by HPLC with electrochemical detection (HPLC/EC) as described previously (45). To determine repair kinetics, cells were treated for 30 min with 20 mM KBrO$_3$, and at each time point, 1×10^6 cells

were removed from dishes, DNA extracted and levels measured as described earlier in the text.

RESULTS

Characterization of wild-type and Q338H MUTYH recombinant proteins

The MUTYH glycosylase activity of the Q338H variant was compared with the wild-type one using recombinant proteins. The Q338H variant and the wild-type MUTYH proteins, expressed in *E. coli* strain BL21 Codon Plus and purified as already described (18), were identified as a major band of 105 kDa by Coomassie staining after separation on a 4–12% SDS–PAGE (Supplementary Figure S1).

To properly compare the enzymatic activity of the wild-type and variant protein, the active fraction of MUTYH preparations was evaluated (17,18). Multiple turnover kinetics were performed with the DNA substrate concentration in excess with respect to the MUTYH concentration. In these conditions, MUTYH shows a biphasic kinetics behaviour, and after a rapid pre-steady state burst (related to the DNA–glycosylase reaction), a slow linear increase of product formation is observed, which is related to a limited turnover of the protein (47,18) (Figure 1A). The active yield of the proteins and the kinetics parameters were evaluated in several protein preparations and are reported in Table 1.

The catalytic constants were evaluated by single-turnover experiments ([MUTYH]$\gg$[DNA]) (Figure 1B). Duplex DNA substrate containing a single 8-oxodG:A
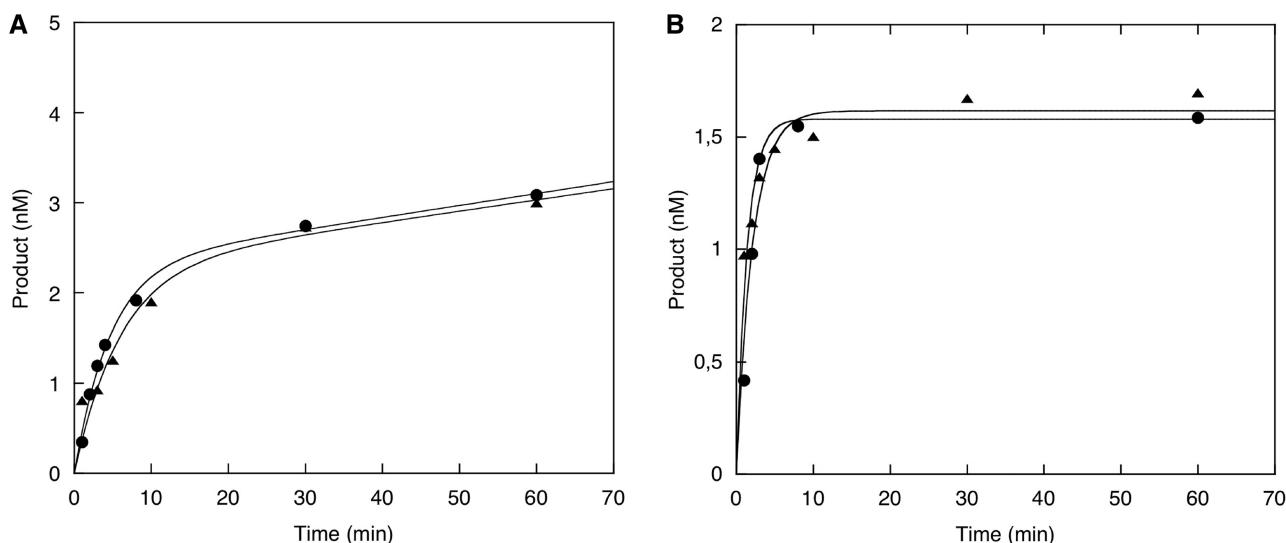

Figure 1. Comparison of the DNA–glycosylase activity of recombinant wild-type and Q338H MUTYH proteins. (**A**) Representative plot of product formation under multiple turnover conditions obtained by reacting the 6-FAM–DNA substrate (10 nM) with 2 nM wild-type (circle) or Q338H MUTYH (triangle) in 10 μl reaction buffer at 37°C. Aliquots were withdrawn at different times ranging from 30 s to 60 min and processed by alkali treatment. Reaction products were analysed by electrophoresis on a 20% polyacrylamide–urea gel in 1× Tris-borate-EDTA (TBE) at 500 V for 3 h. Fluorescent bands, visualized by Typhoon 9200 Gel Imager, were quantified using the public domain NIH *Image J* software. The concentration of the cleaved product (nM) was plotted as a function of time and data fitted by Kaleidagraph software. The active fraction of both wild-type and Q338H MUTYH were evaluated by fitting data to Equation (1). (**B**) Representative plot of product formation under single-turnover condition. DNA (2 nM) was reacted with 20 nM active MUTYH proteins in 10 μl of reaction buffer at 37°C. Data were fitted to Equation (2) and processed as described earlier in the text.

Table 1. Evaluation of active protein concentration and determination of rate constants for wild-type and Q338H

Protein	Full-length protein nM	Active protein nM	k_L min^{-1} nM	k_{ST} min^{-1}
Wild-type	678; 474; 52	275; 27.5; 7.5	0.015 ± 0.006	2.14 ± 0.004
Q338H	216; 310; 176	1.5; 26.4; 10	0.020 ± 0.009	2.01 ± 0.012

mismatch (2 nM) was incubated with the MUTYH protein (20 nM) at 37°C, and aliquots, withdrawn at different reaction times ranging from 30 s to 60 min, were further processed by alkaline treatment. Time course kinetics of wild-type or Q338H MUTYH activity were analysed by plotting the reaction product concentration as a function of time and fitting the curves to a single exponential equation [Equation (2)]. The rate constants for wild-type and Q338H MUTYH were identical within experimental errors (Table 1).

The removal of adenine base from an 8-oxodG:A DNA substrate is the initial step in the repair process; then other proteins are recruited to complete the removal of oxidative damage. APE1, the protein involved in the incision step at the abasic site produced by MUTYH, has been shown to affect MUTYH functional activity by modifying its turnover (20,48,49). When time course kinetics were carried out in the presence of APE1, the rate of glycosylase-mediated base removal by the wild-type MUTYH protein was enhanced (Figure 2A), with a 2-fold increase in product formation. Only a slight difference (1.5-fold increase of final product concentration) in comparison with the wild-type protein was observed when APE1 was incubated in the presence of Q338H MUTYH (Figure 2B). In contrast, and in agreement with other authors (20,47), when the stimulating effect of APE1 was tested on the DNA glycosylase activity of the G396D MUTYH variant, the time course kinetics were found to be substantially unmodified (Figure 2C).

To characterize the association/dissociation features of these proteins to the DNA substrate, kinetic parameters of the interaction with the 8-oxodG:A substrate were measured by SPR (18). Representative sensorgrams, corrected for the blank values, obtained after injection of serial dilutions of the wild-type and Q338H proteins on the immobilized DNA, are shown in Figure 3A and B. The association rate constant (k_{on}), the dissociation rate constant (k_{off}) and the dissociation constant (K_D) were evaluated by 1:1 Langmuir analysis. No significant differences in the binding affinity to the DNA substrate were observed between the wild-type and polymorphic variant (Table 2).

Interaction between wild-type or Q338H variant and the 9–1–1 complex

The IDC region of MUTYH has been demonstrated to interact with the checkpoint sensor 9–1–1 through the HUS1 component of the ternary complex (28). To investigate whether the Q338H substitution affected the binding capacity of the MUTYH protein to the 9–1–1 complex, we performed pull-down assays using nuclear
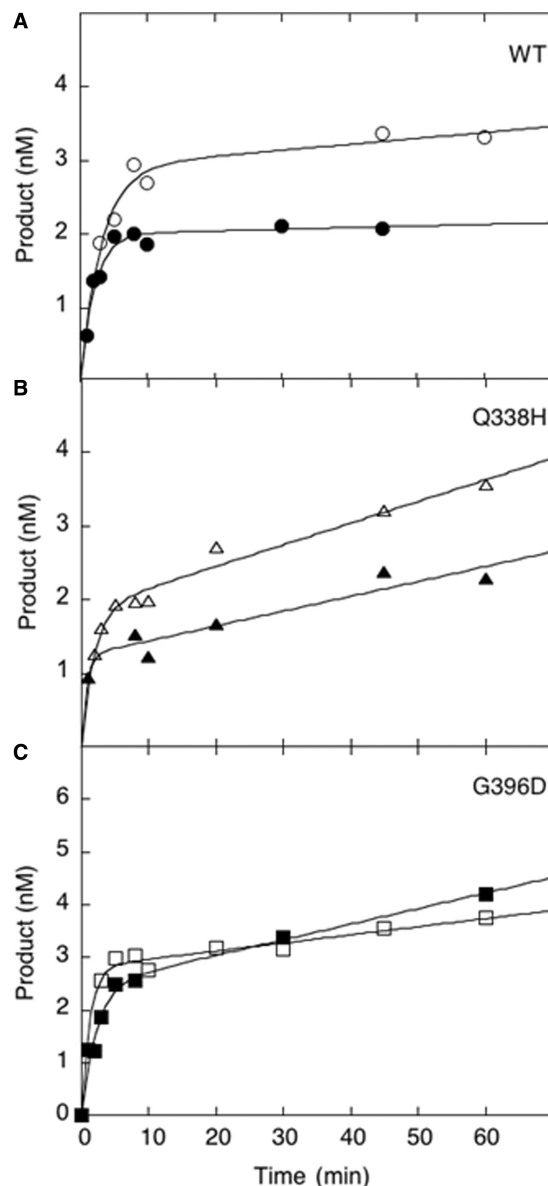

Figure 2. APE1 stimulation assay. Representative plot of product formation as function of time obtained by reacting the DNA substrate (10 nM) with wild-type, Q338H or G396D MUTYH proteins (5 nM) and 1 U of APE1. Reaction products were analysed on a 20% polyacrylamide–urea gel in 1 × TBE at 500 V for 3 h. Fluorescent bands, visualized by Typhoon 9200 Gel Imager, were quantified using the public domain NIH *Image J* software. The concentration of the cleaved product (nM) was plotted as a function of time and data fitted by Kaleidagraph software. (**A**) Wild-type MUTYH; (**B**) Q338H; and (**C**) G396D (empty and full symbols indicate reactions with and without APE1, respectively).

extracts from HeLa cells. The MBP–MUTYH proteins were incubated with HeLa nuclear cell extracts, and the interacting partners, captured by anti-MBP magnetic beads, were subsequently fractionated by SDS–PAGE and analysed by western blot with specific antibodies for RAD9, HUS1 and MUTYH proteins. As shown in the Figure 4A, the components of the 9–1–1 complex present in the nuclear extracts were found to interact with the 105 kDa recombinant MUTYH proteins
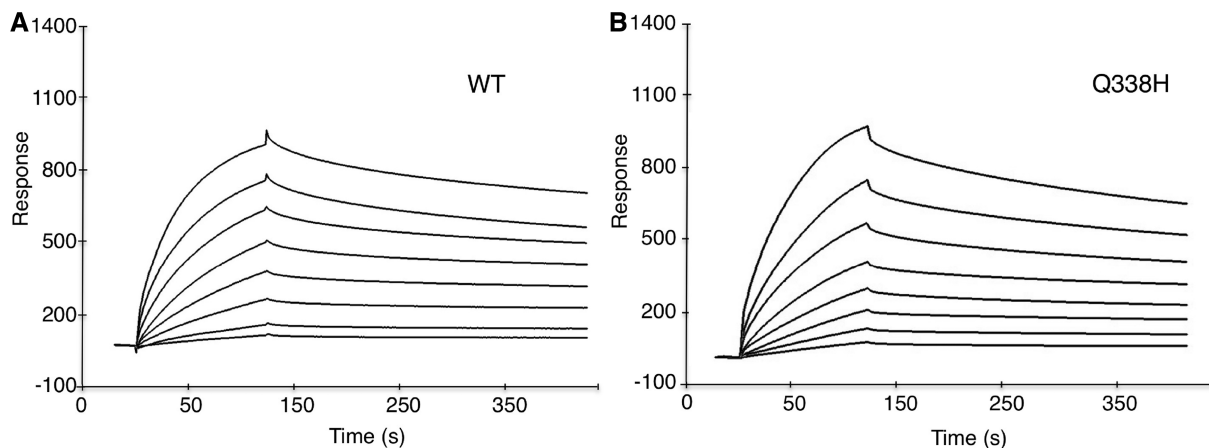
Figure 3. SPR analysis of DNA–MUTYH interaction. Serial dilutions of (**A**) wild-type MUTYH (0.47 μM to 3.67 nM) and (**B**) Q338H MUTYH (0.37 μM to 2.65 nM) were injected onto an 8-oxodG:A substrate, immobilized on a SA chip, at 30 μl/min. The association phase was allowed for 1800 s followed by a 300 s time delay, before starting the washing procedure. The response was recorded as a function of time. The derived kinetics parameters are provided in Table 2.

Table 2. DNA-binding kinetics parameters of wild-type and Q338H variant MUTYH

Protein	K_D (M)	k_{on} (M^{-1}s^{-1})	k_{off} (s^{-1})
Wild-type	6.20 E-09	(1.21 ± 0.01) E+05	(6.83 ± 0.02) E-04
Q338H	8.86 E-09	(1.06 ± 0.01) E+05	(7.84 ± 0.03) E-04

(the 55 kDa endogenous protein of HeLa cells is not shown in the Figure). Calculation of the relative ratios of RAD9/ MUTYH and HUS1/MUTYH proteins indicated that the fractions of RAD9 and HUS1 associated to the Q338H variant were reduced, in comparison with wild-type MUTYH, by >50% and 80%, respectively (Figure 4B). We noticed that MUTYH proteins pulled down also a slower migrating RAD9, possibly corresponding to the hyperphosphorylated form. However, the reduced association was unaffected by inclusion of the minor RAD9 band in the calculation (data not shown).

A similarly decreased interaction of the Q338H variant with the 9–1–1 complex was confirmed by MBP pull-down assays using a purified 9–1–1 complex (Supplementary Figure S2A). When corrected for the MUTYH fraction bound to the beads, a mean reduction of 50% in the binding of RAD9 to the Q338H variant was identified (Supplementary Figure S2B). In conclusion, both using a purified 9–1–1 complex or the endogenous cellular one, we were able to demonstrate that the Q338H variant is partially defective in its interaction with this replication sensor.

Expression of wild-type and Q338H MUTYH cDNAs in $Mutyh^{-/-}$ MEFs and sensitivity to oxidant treatment

Immortalized MEFs from Mutyh-null mice were transfected with the pYMv200 expression vector containing either wild-type or Q338H MUTYH cDNA. Cells transfected with an empty vector were used as a control (46). MUTYH expression levels were analysed by western blotting using a MUTYH-specific antibody, and similar expression levels were found in Q338H- and wild-type–expressing MEFs (Supplementary Figure S3). No signal was detected in $Mutyh^{-/-}$ cells or in $Mutyh^{-/-}$ expressing an empty vector.

Cell survival was measured by clonal assays in cells transfected with either wild-type or Q338H MUTYH cDNAs after exposure to increasing concentrations of KBrO$_3$ (Figure 5). Q338H-expressing MEFs showed hypersensitivity to this oxidant when compared with cells complemented with wild-type cDNA (Figure 5). Interestingly, this hypersensitivity was even more pronounced than that observed in Mutyh-null cells.

Flow cytometry was used to investigate how KBrO$_3$ treatment affects cell cycle progression. After 30 min exposure to KBrO$_3$, cells were harvested at different time points, stained with propidium iodide and analysed by FACS. When wild-type cells were treated with 30 mM KBrO$_3$, an arrest in the progression through the S phase was visible 6 h after the end of the treatment, whereas at 24 and 48 h, the normal progression was restored and no differences with an untreated control population were observed. Examples of FACS profiles and their quantitative evaluation are shown in Figure 6A and B. In Q338H-expressing MEFs, in contrast, a much more pronounced arrest in the progression through the S phase was visible at 6 h. The S phase arrest seems to be relieved at 24 h with an accumulation of the cell population in the G$_2$ phase. At 48 h, a partial restoration of the normal progression of the cell cycle was observed.

At higher concentration of KBrO$_3$ (60 mM), wild-type cells slow down S phase progression and accumulate in the G$_2$ phase after 24 h. Later on (48 h), the vast majority of cells are arrested in the S phase. In contrast, the whole KBrO$_3$-treated population of Q338H MEFs is permanently blocked in the S phase already at 24 h.

We conclude that perturbation of cell cycle progression induced by oxidant exposure is more pronounced in MEFs expressing the Q338H variant when compared with wild-type cells. The major difference between wild-type and the variant cell behaviour is a more pronounced delay of the damaged Q338H cell population in the transit
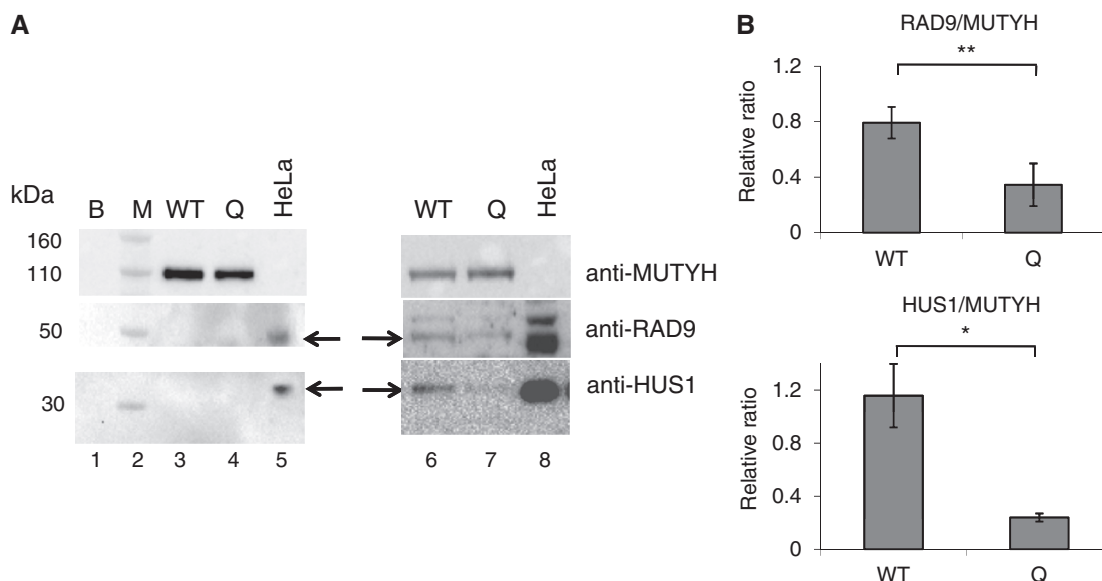
Figure 4. MBP-pull down assay. The physical interaction between MBP–MUTYH and the RAD9 and HUS1 components of the 9–1–1 complex was revealed by immunomagnetic isolation of MBP–MUTYH by using anti-MBP beads. Pull-down proteins were separated by SDS–PAGE, blotted and analysed with MUTYH-, RAD9- and HUS1-specific antibodies. (**A**) Nuclear extracts incubated in absence (lane 1) or in presence of wild-type (lane 6) and Q338H MBP–MUTYH (lane 7) and pulled down. Lanes 3 and 4, beads-immobilized wild-type and Q338H proteins; lanes 5 and 8, 30 μg of nuclear extract. In lane 2, a molecular weight marker (M) has been visualized by merging the colorimetric scan of the same membrane by Image Lab™ software. Evaluation of relative levels of RAD9 and HUS1 bound to wild-type and Q338H MBP–MUTYH. Data are the mean ± SD of three experiments. The asterisks (*) and (**) indicate significant differences by Student's *t*-test ($P < 0.05$ and $P < 0.01$, respectively).
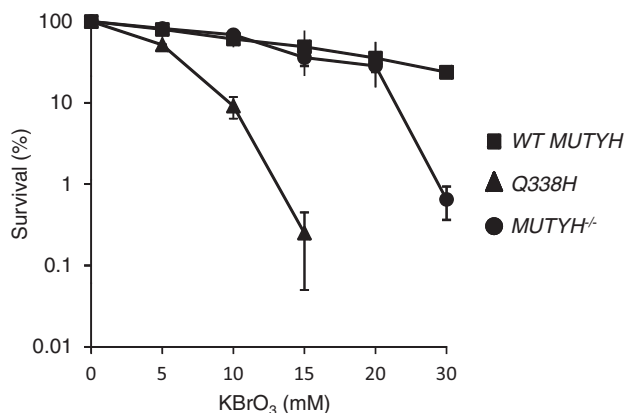

Figure 5. Sensitivity to KBrO$_3$ of *Mutyh*$^{-/-}$ MEFs complemented with wild-type (squares) and Q338H (triangles) *MUTYH* cDNA or without the cDNA insert (circles). Survival was determined by clonal assays after 30 min exposure to increasing concentration of KBrO$_3$. Data represent the mean ± SD of three independent determinations. Data for *Mutyh*$^{-/-}$ cells are taken from the study conducted by Maltore *et al.* (46).

through the S and G$_2$ phase of the cell cycle. It is tempting to speculate that variant cells experiencing severe and unrepairable DNA damage are unable to recover from the S phase arrest, especially at the highest dose, and progress into cell death. These results are consistent with our data on the clonogenic ability of the Q338H cells and their hypersensitivity to oxidative damage.

Steady-state levels and repair capacity of DNA in wild-type and Q338H-expressing MEFs

We have previously shown that several mutations in the *MUTYH* gene are associated with increased basal levels of 8-oxodG in genomic DNA (46). This was also the case for Q338H-expressing MEFs, in which steady-state levels of the oxidized purine were 2-fold higher than in *Mutyh*$^{-/-}$ cells complemented with wild-type *MUTYH* cDNA ($P = 0.01$) (Figure 7A). This increase in DNA oxidations is well within those observed in cell lines expressing mutant *MUTYH* cDNAs (46).

We have previously shown that loss of MUTYH or expression of human mutant proteins is also associated with a defective removal of 8-oxodG from DNA with almost a doubling in the half-life of the lesion (46). After exposure to KBrO$_3$, repair of DNA was then compared in *Mutyh*$^{-/-}$ MEFs complemented with either wild-type or Q338H *MUTYH* cDNA, as well as in the parental cell line. Cells expressing the MUTYH Q338H variant showed DNA repair kinetics much slower than those observed in *Mutyh*$^{-/-}$-corrected cells (Figure 7B), with a half-life of the lesion similar to that observed in *Mutyh*$^{-/-}$ cells (46). The residual absolute 8-oxo-dG levels for untransfected, wild-type– and Q338H-complemented MEFs are also shown in Supplementary Figure S4.

These data indicate that expression of the Q338H variant is associated with defective removal of 8-oxodG:A mismatches identified both at steady-state levels and after exposure to an oxidative stress.

DISCUSSION AND CONCLUSION

Cells have evolved several related mechanisms to neutralize the oxidizing effects of endogenous and exogenous agents on nucleic acids. During replication, the insertion of the adenine base opposite an 8-oxodG template is counteracted by MUTYH DNA–glycosylase, which
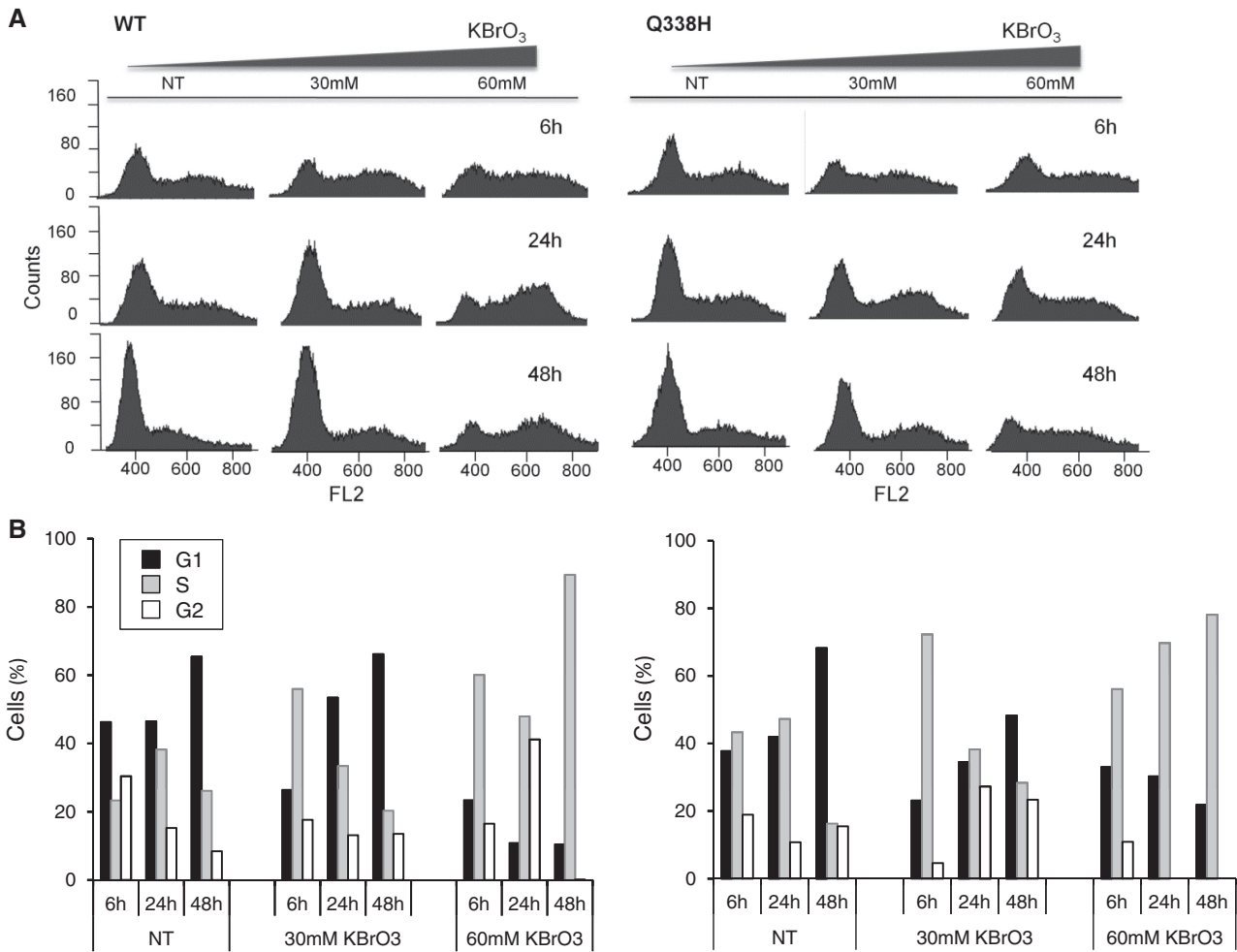
Figure 6. Cell cycle progression in wild-type and Q338H-expressing MEFs after exposure to KBrO$_3$. (**A**) Cytofluorimetric analysis of cell cycle of *Mutyh$^{-/-}$* MEFs expressing wild-type and Q338H cDNAs. Cells were exposed to 30 and 60 mM KBrO$_3$ and sampled for analysis at the indicated time points. (**B**) The panels show the percentage of cells in G$_1$ (black bars), S (grey bars) and G$_2$ (open bars) phases of the cell cycle.
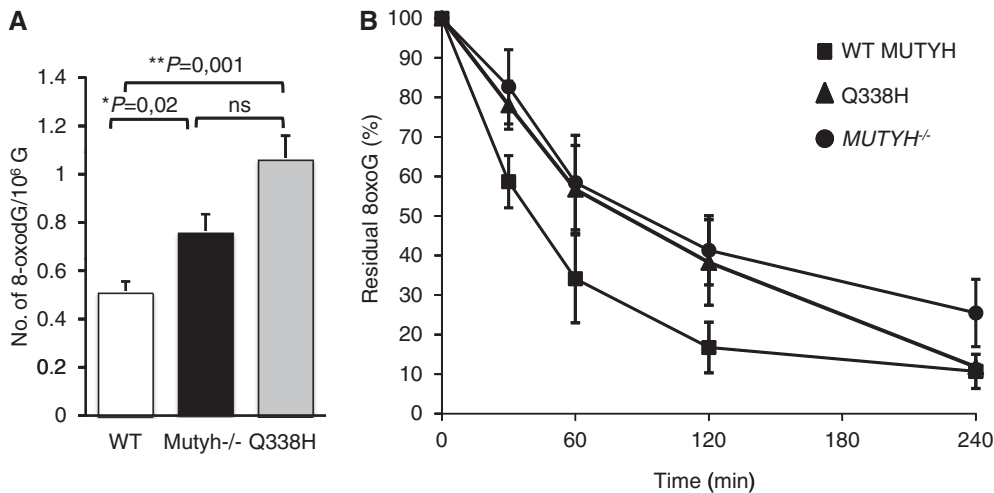

Figure 7. Steady-state levels and repair kinetics of DNA 8-oxodG. (**A**) Steady-state levels of DNA 8-oxodG in *Mutyh$^{-/-}$* (black bar), *Mutyh$^{-/-}$* MEFs complemented with wild-type (open bar) and Q388H (grey bar) *MUTYH* cDNA. Data are the mean ± SD of four experiments. (**B**) Levels of DNA 8-oxodG were measured at the indicated time points in *Mutyh$^{-/-}$* (circles) and *Mutyh$^{-/-}$* MEFs complemented with wild-type (squares) and Q388H (triangles) *MUTYH* cDNA, after 30 min treatment with 20 mM KBrO$_3$. Data are the mean ± SD of two experiments. *P*-values were calculated by Student's *t*-test.

removes the mismatched base. In addition to DNA–glycosylase activity, MUTYH exerts a co-ordinating role of other players at the lesion site. Different functional domains of MUTYH are involved in the interaction with several replication and or repair proteins, as well as with the replication checkpoint 9–1–1 complex. Although the most common MUTYH variants identified in MAP patients display loss of catalytic activity, it is plausible that a defective MUTYH phenotype might also depend on mutations that affect protein–protein interactions.

Here, we report a systematic study that indicates that the substitution of the Q338 residue in the MUTYH variant does not modify the DNA-binding capacity or the DNA–glycosylase activity of the recombinant purified protein in the *in vitro* assays. These results are in agreement with other studies, showing that the variant recombinant protein has wild-type glycosylase activity, in the buffer conditions we used (41,42) and can complement the mutator phenotype of an *E. coli MutM Muty* strain (41). A novel observation is the reduced ability of this MUTYH variant to bind the 9–1–1 complex demonstrated by pull-down assays. The mutation at 338 residue occurs in the IDC region, which is missing in bacteria, is conserved in eukaryotes and is largely unstructured. This latter feature, which is frequently found in other BER proteins, seems to be of relevance in regulating the formation of multi-protein complexes. Indeed, the IDC has been reported to interact with the HUS1 subunit of the 9–1–1 complex (28,29), and the extent of interaction is affected by mutations or deletions in this region (29). Thus, when the *Schizosaccharomyces pombe* I261 and E262 residues (equivalent to V329 and E330 of the human MUTYH) were mutated to Ala and Gln, respectively, a defective interaction with the 9–1–1 complex was identified (28). Our results on the Q338H variant extend these observations to a variant present in the human population and confirm the importance of this region in modulating protein–protein interactions.

Accumulation of 8-oxodG in DNA and slow removal of the oxidized base from the genome in Q338H expressing-*Mutyh*$^{-/-}$ MEFs is consistent with an acknowledged phenotype associated with loss of MUTYH enzymatic function (46). The hypersensitivity to KBrO$_3$ treatment identified in Q338H expressing-Mutyh$^{-/-}$ MEFs is also a characteristic of MUTYH-defective cells (46). However, although the extent of the repair defect in the variants is similar to that observed in *Mutyh*-null cells (46), more dramatic consequences on oxidant-induced cell killing were observed in cells expressing the Q338H allele. Is the defective interaction of the Q338H variant with the 9–1–1 complex responsible for these enhanced effects on cell death? Indeed, the 9–1–1 complex has been involved in recruiting several DNA repair enzymes, suggesting that lack of proper interaction hampers a correct localization of the repair protein on damaged DNA (30–40). One possibility would be that the Q338H variant acts as a dominant negative mutant resulting in the accumulation of toxic repair intermediate(s). This could be consistent with the observed enhanced and sustained S phase arrest of the Q338H-expressing cells in comparison with the transient accumulation in the S-phase of the cell cycle of the wild-type cells.

We propose that the coordination of MUTYH with S-phase checkpoint factors is essential for proper DNA repair and is one of the major determinants in avoiding cell death.

During the preparation of this article, Raetz *et al.* (42) reported that the repair capacity of Q338H-expressing MEFs, as measured by a plasmid-based fluorescent reporter, is significantly lower than wild-type controls. In particular, the Q338H variant exhibited reduced repair levels that approached those of the well-characterized Y179C and G396D cancer variants (42). Our data nicely complement these observations and demonstrate that in an *in vivo* cellular context, together with defects in the intrinsic adenine glycosylase activity, changes affecting protein–protein interactions might also influence DNA repair capacity.

Although the Q338H variant was frequently identified among Japanese familial adenomatous poliposis (FAP) patients (21), the authors considered this polymorphism unrelated to phenotypic features of FAP. Similarly, no significant differences in genotype frequencies were identified in relatively limited series of controls and cases (11,12,50). It is interesting that the Q338H variant has been reported to confer, in homozygous status, a small increased risk (odds ratio 1.52, confidence interval = 1.06–2.17) of rectal cancer, leading the authors to propose that this might be a low-penetrance allele (50). In addition, it has been suggested that compound heterozygotes of pathogenic MUTYH mutations and the Q338H variant might be at increased risk for mild polyposis or colorectal cancer (CRC) (51).

In view of the ongoing efforts to assess and refine CRC risk estimates associated with mono-allelic MUTYH variants (52), our data suggest that the Q338H mutation should not be dismissed as a neutral polymorphic variant. Future studies of MUTYH enzymatic activity in lymphoblastoid cell lines derived from MAP patients harbouring the Q338H variant in combination with acknowledged pathogenic mutations MUTYH will clarify this point.

SUPPLEMENTARY DATA

Supplementary Data are available at NAR Online: Supplementary Figures 1–4.

ACKNOWLEDGEMENTS

FUNDING

REFERENCES

1. Barnes,D.E. and Lindahl,T. (2004) Repair and genetic consequences of endogeneous DNA base damage in mammalian cells. *Annu. Rev. Genet.*, **38**, 445–476.
2. Fortini,P. and Dogliotti,E. (2006) Base damage and single-strand break repair: mechanisms and functional significance of short and long-patch repair subpathways. *DNA Repair*, **6**, 398–409.
3. Slupska,M.M., Luther,W.M., Chiang,J.H., Yang,H. and Miller,J.H. (1999) Functional expression of hMYH, a human homolog of the *Escherichia coli* MutY protein. *J. Bacteriol.*, **181**, 6210–6213.
4. Parker,A.R. and Eshleman,J.R. (2003) Human MutY: gene structure, protein functions and interactions, and role in carcinogenesis. *Cell. Mol. Life Sci.*, **60**, 2064–2083.
5. Parker,A., Gu,Y., Mahoney,W., Lee,S.H., Singh,K.K. and Lu,A.L. (2001) Human homolog of the MutY repair protein (hMYH) physically interacts with proteins involved in long patch DNA base excision repair. *J. Biol. Chem.*, **276**, 5547–5555.
6. Balakrishanan,L., Brandt,P.D., Lindsey-Boltz,L.A., Sancar,A. and Bambara,R.A. (2009) Long patch base excision repair proceeds via coordinated stimulation of the multienzyme DNA repair complex. *J. Biol. Chem.*, **284**, 15158–15172.
7. van Loon,B. and Hübscher,U. (2009) An 8-oxo-guanine repair pathway coordinated by MUTYH glycosylase and DNA polymerase lambda. *Proc. Natl Acad. Sci. USA*, **106**, 18201–18206.
8. Boldogh,I., Milligan,D., Lee,M.S., Bassett,H., Lloyd,R.S. and McCullough,A.K. (2001) hMYH cell cycle dependent expression, subcellular localization and association with replication foci: evidence suggesting replication-coupled repair of adenine:8-oxoguanine mispairs. *Nucleic Acids Res.*, **29**, 2802–2809.
9. Gu,Y., Parker,A., Wilson,T.M., Bai,H., Chang,D.Y. and Lu,A.L. (2002) Human MutY homolog, a DNA glycosylase involved in base excision repair, physically and functionally interacts with mismatch repair proteins human MutS homolog 2/human MutS homolog 6. *J. Biol. Chem.*, **277**, 11135–11142.
10. Chang,D.Y. and Lu,A.L. (2002) Functional interaction of MutY homolog with proliferating cell nuclear antigen in fission yeast *Schizosaccharomyces pombe*. *J. Biol. Chem.*, **277**, 11853–11858.
11. Al-Tassan,N., Chmiel,N.H., Maynard,J., Fleming,N., Livingston,A.L., Williams,G.T., Hodges,A.K., Davies,D.R., David,S.S., Sampson,J.R. *et al.* (2002) Inherited variants of MYH associated with somatic G:C—>T:A mutations in colorectal tumors. *Nat. Genet.*, **30**, 227–232.
12. Sieber,O.M., Lipton,L., Crabtree,M., Heinimann,K., Fidalgo,P., Phillips,R.K., Bisgaard,M.L., Orntoft,T.F., Aaltonen,L.A., Hodgson,S.V. *et al.* (2003) Multiple colorectal adenomas, classic adenomatous polyposis, and germ-line mutations in MYH. *N. Engl. J. Med.*, **348**, 791–799.
13. Out,A.A., Tops,C.M., Nielsen,M., Weiss,M.M., van Minderhout,I.J., Fokkema,I.F., Buisine,M.P., Claes,K., Colas,C., Fodde,R. *et al.* (2010) Leiden open variation database of the MUTYH gene. *Hum. Mutat.*, **31**, 1205–1215.
14. Bai,H., Jones,S., Guan,X., Wilson,T.M., Sampson,J.R., Cheadle,J.P. and Lu,A.L. (2005) Functional characterization of two human MutY homolog (hMYH) missense mutations (R227 and V232F) that lie within the putative hMSH6 binding domain and are associated with MYH polyposis. *Nucleic Acids Res.*, **33**, 597–604.
15. Bai,S., Grist,J., Gardner,G., Suthers,G., Wilson,T.M. and Lu,A.L. (2007) Functional characterization of human MutY homolog (hMYH) missense mutation (R231L) that is linked with hMYH-associated polyposis. *Cancer Lett.*, **250**, 74–81.
16. Ali,M., Kim,H., Cleary,S., Cupples,C., Gallinger,S. and Bristow,R. (2008) Characterization of mutant MUTYH proteins associated with familial colorectal cancer. *Gastroenterology*, **135**, 499–507.
17. Kundu,S., Brinkmeyer,M.K., Livingston,A.L. and David,S.S. (2009) Adenine removal activity and bacterial complementation with the human MutY homologue (MUTYH) and Y165C, G382D, P391L and Q324R variants associates with colorectal cancer. *DNA Repair*, **8**, 1400–1410.
18. D'Agostino,V.G., Minoprio,A., Torreri,P., Marinoni,I., Bossa,C., Petrucci,T.C., Albertini,A.M., Ranzani,G.M., Bignami,M. and Mazzei,F. (2010) Functional analysis of MUTYH mutated proteins associated with familial adenomatous polyposis. *DNA Repair*, **9**, 700–707.
19. Goto,M., Shinmura,K., Nakabeppu,Y., Tao,H., Yamada,H., Tsuneyoshi,T. and Sugimura,H. (2010) Adenine DNA glycosylase activity of 14 human MutY homolog (MUTYH) variant proteins found in patients with colorectal polyposis and cancer. *Hum. Mutat.*, **31**, E1861–E1874.
20. Pope,M.A., Chmiel,N. and David,S.S. (2005) Insight into the functional consequences of hMYH variants associated with colorectal cancer: distinct differences in the adenine glycosylase activity and the response to AP endonucleases of Y150C and G365D murine MYH. *DNA Repair*, **4**, 315–325.
21. Ushijima,Y., Tominaga,Y., Miura,T., Tsuchimoto,D., Sakumi,K. and Nakabeppu,Y. (2005) A functional analysis of the DNA glycosylase activity of mouse MUTYH protein excising 2-hydroxyadenine opposite guanine in DNA. *Nucleic Acids Res.*, **33**, 672–682.
22. Yanaru-Fujisawa,R., Matsumoto,T., Ushijima,Y., Esaki,M., Hirahashi,M., Gushima,M., Yao,T., Nakabeppu,Y. and Iida,M. (2008) Genomic and functional analyses of MUTYH in Japanese patients with adenomatous polyposis. *Clin. Genet.*, **73**, 545–553.
23. Alhopuro,P., Parker,A., Lehtonen,R., Enholm,S., Jarvinen,H.J., Mecklin,J.P., Karhu,A., Eshleman,J.R. and Aaltonen,L.A. (2005) A novel functionally deficient MYH variant in individuals with colorectal adenomatous polyposis. *Hum. Mutat.*, **26**, 393–402.
24. Parker,A.R., Sieber,O.M., Shi,C., Hua,L., Takao,M., Tomlinson,I.P. and Eshleman,J.R. (2005) Cells with pathogenic biallelic mutations in the human MUTYH gene are defective in DNA damage binding and repair. *Carcinogenesis*, **26**, 2010–2018.
25. Bartek,J., Lukas,C. and Lukas,J. (2004) Checking on DNA damage in S phase. *Nat. Rev. Mol. Cell Biol.*, **5**, 792–804.
26. Dorè,A.S., Kilkenny,M.L., Rzechorzek,N.J. and Pearl,L.H. (2009) Crystal structure of the RAD9-RAD1-HUS1 DNA damage checkpoint complex-implications for clamp loading and regulation. *Mol. Cell.*, **34**, 735–745.
27. Sohn,S.Y. and Cho,Y. (2009) Crystal structure of human rad9-hus1-rad1 clamp. *J. Mol. Biol.*, **390**, 490–502.
28. Shi,G., Chang,D.Y., Cheng,C.C., Cuan,X., Venclovas,C. and Lu,A.L. (2006) Physical and functional interactions between MutY glycosylase homologue (MYH) and checkpoint proteins RAD9-RAD1-HUS1. *Biochem. J.*, **400**, 53–62.
29. Luncsford,P.J., Chang,D.Y., Shi,G., Bernstein,J., Madabushi,A., Patterson,D.N., Lu,A.L. and Toth,E.A. (2010) A structural hinge in eukaryotic MUTY homologues mediates catalytic activity and RAD9-RAD1-HUS1 checkpoint complex interactions. *J. Mol. Biol.*, **403**, 351–370.
30. Gembka,A., Toueille,M., Smirnova,E., Poltz,R., Ferrari,E., Villani,G. and Hubscher,U. (2007) The checkpoint clamp, RAD9-RAD1-HUS1 complex, preferentially stimulates the activity of apurinic/apyrimidinic endonuclease 1 and DNA polymerase β in long patch base excision repair. *Nucleic Acids Res.*, **35**, 2596–2608.
31. Toueille,M., El-Andaloussi,N., Frouin,I., Freire,R., Funk,D., Shevelev,I., Friedrich-Heineken,E., Villani,G., Hottiger,M.O. and Hubscher,U. (2004) The human RAD9/RAD1/HUS1 damage sensor clamp interacts with DNA polymerase beta and increases its DNA substrate utilization efficiency: implications for DNA repair. *Nucleic Acids Res.*, **32**, 3316–3324.
32. Friedrich-Heineken,E., Toueille,M., Tannler,B., Burki,C., Ferrari,E., Hottiger,M.O. and Hubscher,U. (2005) The two DNA clamps RAD9/RAD1/HUS1 complex and proliferating cell nuclear antigen differentially regulate flap endonuclease 1 activity. *J. Mol. Biol.*, **353**, 980–989.

33. Wang,W., Brandt,P., Rossi,M.L., Lindsey-Boltz,L., Podust,V., Fanning,E., Sancar,A. and Bambara,R.A. (2004) The human RAD9-RAD1-HUS1 checkpoint complex stimulates flap endonuclease1. *Proc. Natl Acad. Sci. USA*, **101**, 16762–16767.

34. Smirnova,E., Toueille,M., Markkanen,E. and Hubscher,U. (2005) The human checkpoint sensor and alternative DNA clamp RAD9-RAD1-HUS1 modulates the activity of DNA ligase I, a component of the long-patch base excision repair machinery. *Biochem. J.*, **389**, 13–17.

35. Wang,W., Lindsey-Boltz,L.A., Sancar,A. and Bambara,R.A. (2006) Mechanism of stimulation of human DNA ligase I by the RAD9-RAD1-HUS1 checkpoint complex. *J. Biol. Chem.*, **281**, 20865–20872.

36. Park,M.J., Park,J.H., Hahm,S.H., Ko,S.I., Lee,Y.R., Chung,J.H., Sohn,S.Y., Cho,Y., Kang,L.W. and Han,Y.S. (2009) Repair activities of human 8-oxoguanine DNA glycosylase are stimulated by the interaction with human checkpoint sensor RAD9-RAD1-HUS1 complex. *DNA Repair*, **8**, 1190–1200.

37. Guan,X., Madabushi,A., Chang,D.Y., Fitzgerald,M.E., Shi,G., Drohat,A.C. and Lu,A.L. (2007) The human checkpoint sensor RAD9-RAD1-HUS1 interacts with and stimulates DNA repair enzyme TDG glycosylase. *Nucleic Acids Res.*, **35**, 6207–6218.

38. Guan,X., Bai,H., Shi,G., Theriot,C.A., Hazra,T.K., Mitra,S. and Lu,A.L. (2007) The human checkpoint sensor RAD9-RAD1-HUS1 interacts with and stimulates Neil1 glycosylase. *Nucleic Acids Res.*, **35**, 2463–2472.

39. Wu,X., Shell,S.M. and Zou,Y. (2005) Interaction and colocalization of Rad9/Rad1/Hus1 checkpoint complex with replication protein A in human cells. *Oncogene*, **24**, 4728–4735.

40. He,W., Zhao,Y., Zhang,C., An,L., Hu,Z. and Lui,Y. (2008) RAD9 plays an important role in DNA mismatch repair through physical interaction with MLH1. *Nucleic Acids Res.*, **36**, 6406–6417.

41. Shinmura,K., Yamaguchi,S., Saitoh,T., Takeuchi-Sasaki,M., Kim,S.R., Nohmi,T. and Yokota,J. (2000) Adenine excisional repair function of MYH protein on the adenine:8-hydroxyguanine base pair in double-stranded DNA. *Nucleic Acids Res.*, **28**, 4912–4918.

42. Raetz,A.G., Xie,Y., Kundu,S., Brinkmeyer,M.K., Chang,C. and David,S.S. (2012) Cancer-associated variants and a common polymorphism of MUTYH exhibit reduced repair of oxidative DNA damage using a GFP-based assay in mammalian cells. *Carcinogenesis*, **33**, 2301–2309.

43. Fromme,J.C., Banerjee,A., Huang,S.J. and Verdine,G. (2004) Structural basis for removal of adenine mispaired with 8-oxoguanine by MutY adenine DNA glycosylase. *Nature*, **427**, 652–656.

44. Klungland,A., Rosewell,I., Hollenbach,S., Larsen,E., Daly,G., Epe,B., Seeberg,E., Lindahl,T. and Barnes,D.E. (1999) Accumulation of premutagenic DNA lesions in mice defective in removal of oxidative base damage. *Proc. Natl Acad. Sci. USA*, **96**, 13300–12305.

45. Russo,M.T., De Luca,G., Casorelli,I., Degan,P., Molatore,S., Barone,F., Mazzei,F., Pannellini,T., Musiani,P. and Bignami,M. (2009) Role of MUTYH and MSH2 in the control of oxidative DNA damage, genetic instability and tumorigenesis. *Cancer Res.*, **69**, 4372–4379.

46. Molatore,S., Russo,M.T., D'Agostino,V.G., Barone,F., Matsumoto,Y., Albertini,A.M., Minoprio,A., Degan,P., Mazzei,F., Bignami,M. et al. (2010) MUTYH mutations associated with familial adenomatous polyposis: functional characterization by a mammalian cell-based assay. *Hum. Mutat.*, **31**, 159–166.

47. Porello,S.L., Leyes,A.E. and David,S.S. (1998) Single-turnover and pre-steady-state kinetics of the reaction of the adenine glycosylase MutY with mismatch-containing DNA substrates. *Biochemistry*, **37**, 14756–14764.

48. Tominaga,Y., Ushijima,Y., Tsuchimoto,D., Mishima,M., Shirakawa,M., Hirano,S., Sakumi,K. and Nakabeppu,Y. (2004) MUTYH prevents OGG1 or APEX1 from inappropriately processing its substrate or reaction product with its C-terminal domain. *Nucleic Acids Res.*, **32**, 3198–3211.

49. Yang,H., Clendenin,W.M., Wong,D., Demple,B., Slupska,M.M., Chiang,J.H. and Miller,J.H. (2001) Enhanced activity of adenine-DNA glycosylase (Myh) by apurinic/apyrimidinic endonuclease (Ape1) in mammalian base excision repair of an A/GO mismatch. *Nucleic Acids Res.*, **29**, 743–752.

50. Görgens,H., Krüger,S., Kuhlisch,E., Pagenstecher,C., Höhl,R., Schackert,H.K. and Müller,A. (2006) Microsatellite stable colorectal cancers in clinically suspected hereditary nonpolyposis colorectal cancer patients without vertical transmission of disease are unlikely to be caused by biallelic germline mutations in MYH. *J. Mol. Diagn.*, **8**, 178–182.

51. Picelli,S., Zajac,P., Zhou,X.L., Edler,D., Lenander,C., Dalén,J., Hjern,F., Lundqvist,N., Lindforss,U., Påhlman,L. et al. (2010) Common variants in human CRC genes as low-risk alleles. *Eur. J. Cancer.*, **46**, 1041–1048.

52. Casper,M., Plotz,G., Juengling,B., Zeuzem,S., Lammert,F. and Raedle,J. (2012) MUTYH hotspot mutations in unselected colonoscopy patients. *Colorectal Dis.*, **14**, e238–e244.